Development of EPR dosimeters based on SiO_2 for possible use in radiation processing applications

A.A. Abdel-Fattah[a], A.M. Mansour[a], I.I. Bashter[b] and M. Ragab[c]

[a] *National Center for Radiation Research and Technology, AEA, P.O. Box 8029, Nasr City 11371, Cairo, Egypt.*
[b] Faculty of science, zagazig University, Cairo, Egypt.
[C] Higher Technological Institute, 10th of Ramadan city, Egypt.

ABSTRACT

Quartz rods (3×10 mm) for routine use in high-dose radiation applications have been prepared by a simple technique in the laboratory where Quartz powder of two sources $\mathbf{q_1}$ and $\mathbf{q_2}$ each was mixed with molten mixture of paraffin wax and ethylene vinyl acetate copolymer (EVA). The binding mixture of EVA/Paraffin does not exhibit interference or noise in the EPR signal before or after the irradiation. The rods show good mechanical properties for safe and multi-use handling. The rods can be used with good precision in the dose range from 0.1 to 15 kGy for $\mathbf{q_1}$ and from 0.1 to 25 KGy for $\mathbf{q_2}$. The overall uncertainty for calibration using EVAPA rod program was found to be 4.55 % for $\mathbf{q_1}$ and 5.95 % for $\mathbf{q_2}$.The dose response, influence of humidity and temperature during irradiation, energy dependence as well as post-irradiation storage at different conditions are discussed.

Key Words: Quartz, Ethylene Vinyl Acetate, Radiation Dosimetry; EPR.

INTRODUCTION

The quartz/EPR dosimetry system provides a reliable mean for measuring the absorbed dose. It is based on the generation of specific stable radicals in crystalline quartz or via increasing ionising radiation. Identification and determination of the concentration of the generated quartz radicals are performed by electron paramagnetic resonance (EPR) spectroscopy. The concentration of quartz-derived radical is a function of the absorbed dose. EPR technique is non-destructive, so quartz dosimeters can be read out repeatedly and hence could be used for archival purposes.

Several laboratories had successfully developed quartz-EPR dosimeter using different binders [1-10]. Quartz-EPR has been selected by IAEA(International Atomic Energy Authority) as the transfer dosimeter for use in the quality audit service IDAS (International Dose Assurance Service) for several reasons, examples include: near-tissue equivalency, low sensitivity to ambient environment, broad useful dose range, non-destructive analysis, and little fading of the response with time. The disadvantages of quartz/EPR dosimetry system, at that time, were the limited experience of the system and the significant cost of the analysis equipment, namely the electron paramagnetic resonance (EPR) spectrometer.

In the present work, a new simple method for preparation of quartz-EPR rods with a new binding medium has been carried out. The dose response, influence of humidity and temperature during irradiation, energy dependence as well as storage at different conditions are considered.

EXPERIMENTAL PROCEDURES

Materials

Silicon dioxide obtained from different sources:

(1) The commercially available quartz material (silicon dioxide) in crystalline form was crushed to obtain quartz powder (particle size 200-250 μm) with purity 99.5%, ($\mathbf{q_1}$ samples).

(2) The second silicon dioxide obtained from ESR tubes in crystalline form was crushed to obtain quartz powder (particle size 75-112 μm) with purity 99.9%, ($\mathbf{q_2}$ samples).

The two specimens are grinded to fine powder and prepared to quartz rods. Silicon dioxide has a molecular weight of 60.08 and a density of 2.65 g/cm^3 in crystal form, product of* ALDRICH, USA*, hot melt stick adhesive based on ethylene vinyl acetate copolymer (Tec-Bond 232/12, Power Adhesives Limited, England), paraffin wax (congealing point 65-71 ^{o}C, BDH) were used.

Preparation of Quartz rods

For use in routine dosimetry, the adequate mechanical properties of quartz rods are required. To avoid brittleness and to improve the mechanical properties, the quartz content is reduced and ethylene vinyl acetate (EVA) hot melt adhesive is added to paraffin wax.

An equal weight mixture of paraffin wax and EVA hot-melt adhesive was melted in a round bottle at 95 ^{o}C in a water bath. EVA showed a complete compatiblity with paraffin wax. 20 % fine powdered quartz is added to the hot mixture solution and was mechanically stirred for about 10 minutes at the same temperature to obtain a homogeneous mixture. The hot solution is sucked into polypropylene tubes (inner diameter 3 mm) and was left to solidify by cooling. Alanine mixture smaller rod is obtained by removing the polypropylene tube,

and then cutting into rods (3×10 mm dimensions). Three different types of rods were prepared depending on quartz concentration, namely $\mathbf{q_1}$ and $\mathbf{q_2}$ and 20% of quartz. The average mass of the rods for $\mathbf{q_1}$ and $\mathbf{q_2}$ concentrations was found to be 0.0900 ± 0.0970 g for $\mathbf{q_1}$ and 0.0880 ± 0.0950 g for $\mathbf{q_2}$.

Irradiation

Irradiations were carried out gamma radiation in the ^{60}Co gamma chamber (model Issledoleev, product of Russia) which is calibrated using dichromate dosimeters (supplied and measured by National Physical Laboratory, England). The absorbed dose rate at the time of irradiation was about 7.5 kGy/h. Three rods were irradiated together at the central position of the sample chamber using a specially designed holder made from polystyrene to ensure electronic equilibrium.

EPR Measurement

EPR spectra were recorded at ambient temperature with a Bruker EMX spectrometer (X-band); the cavity used was the standard Bruker ER 4102 rectangular cavity. The operating conditions for q_1 are, microwave power=7.989 mW, modulation amplitude=3.00 Gauss, modulation frequency=100 kHz, sweep width=100 Gauss, microwave frequency=9.702 GHz, time constant=163.840 ms, conversion time 40.960 ms and sweep time=40.960 s. The operating conditions for q_2 are, microwave power=0.201 mW, modulation amplitude=4.00 Gauss, modulation frequency=100 kHz, sweep width=300 Gauss, microwave frequency=9.700 GHz, time constant=81.920 ms, conversion time 20.480 ms and sweep time=20.972 s. The bottom of the EPR tube was adjusted at a fixed position to ensure reproducible and accurate positioning of the rods in the sensing zone of the cavity.

EPR spectra were recorded at two orientations for each rod in the EPR cavity (0^o and 90^o degrees). The dose responses of dosimeters were calculated in terms of the average peak-to-peak heights of the two orientations (h_0 and h_{90}) per unit weight of dosimeter and normalized to the receiver gain of the EPR spectrometer. Stability of the EPR spectrometer sensitivity was checked before and after each series of measurement using reference alanine dosimeters irradiated to known doses.

RESULTS AND DISCUSSION

Dose Response

The prepared rods have good mechanical properties adequate for easy and safe handling; although they contain relatively low concentration of quartz. Increasing quartz content increases the brittleness of the rods. Nevertheless, the reduced quartz concentration in the rods has limited effect on the sensitivity of the dosimeter for doses higher than 100 Gy at the used EPR parameters. Figure

(1) shows the EPR spectra for $\mathbf{q_1}$ and $\mathbf{q_2}$ rods before and after irradiation by 25 kGy.

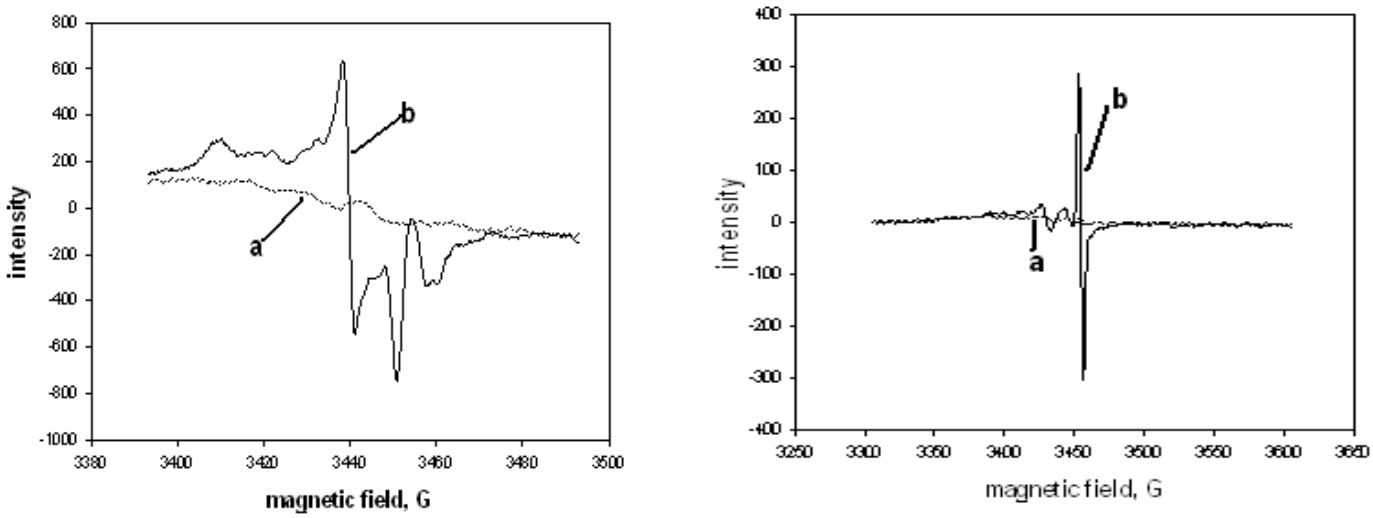

Figure (1). EPR spectra recorded for $\mathbf{q_1}$ and $\mathbf{q_2}$, (a) non-irradiated, (b 20%) irradiated dose 25 KGy

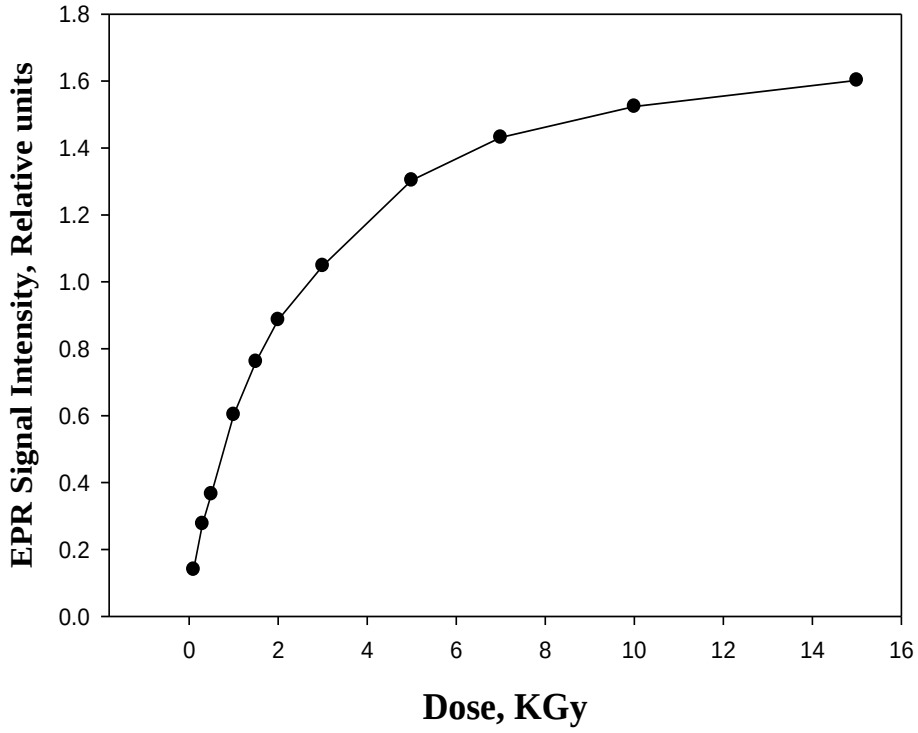

Figure (2). Dose response of irradiated quartz rods (q_1) , at different doses (dose range 0.1-15 kGy)

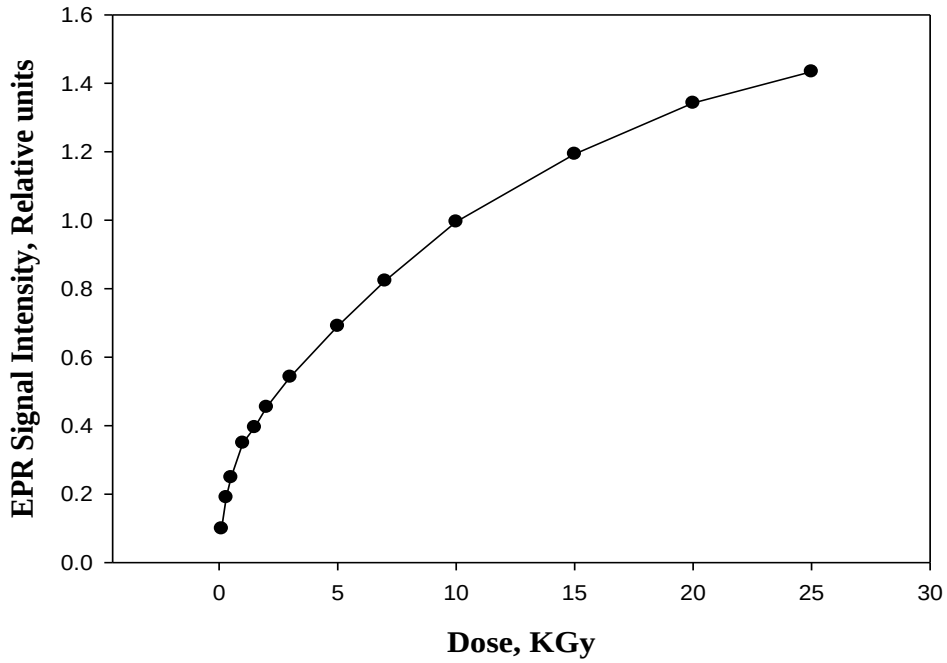

Figure (3). Dose response of irradiated quartz rods (q_2), at different doses (dose range 0.1- 25 kGy)

Fig. 2,3 shows the calibration curves obtained for the irradiated q_1,q_2 rods in terms of average peak-to-peak amplitude normalized to dosimeter mass and receiver gain [peak height/(gain×mass)] versus the absorbed dose over the range from 0.1 to 15 kGy for q_1 and the range of 0.1 to 25 KGy for q_2. Different polynomial functions were tested to fit the different response curves given in Fig. 3, 4. Based on the correlation coefficients and F-statistics values, the best fit was found with the 3rd order polynomial equation. Table 1 shows the constants a, b, c, d and correlation coefficients (r^2) as well as F-statistics values for q_1, q2.

TABLE 1 The constants a,b,c,d,and the Correlation Coefficients (r^2) as well as F-Statistics Values for the 3rd polynomial Fit of q_1,q_2 Response Curves

Dosimeter	*Equations*	*Equation constants*				r^2	*F-stat.*
		a	*B*	*C*	*D*		
q_1	$Y = a + bx + cx^2+dx^3$	0.6443	0.1699	-0.0060	0.0010	0.9986	5052.2960

q_2	$Y = a + bx + cx^2+dx^3$	0.0145	-2e-4	0.3129	0.0630	0.9984	7059.5262

Temperature during Irradiation

The effect of change in temperature during irradiation on the response of q_1, q_2 rods were investigated by irradiating the rods to a dose of 5 kGy at different temperatures (20, 30, 40, and 53 ºC) using isolated thermal baths during irradiation using Styrofoam phantom. The rods were kept at the same temperature for about 1 hour prior to irradiation to maintain thermal equilibrium in the samples during irradiation. Figure 4&5 show the variation in response [peak height/(gain*mass)] as a function of temperature during irradiation relative to that at 30ºC. It can be seen that the response increases linearly with the irradiation temperature in the studied range of temperature. In other words the temperature coefficients at the studied dose level (5 kGy) are equal to 0.6 %ºC^{-1} for q_1 and 0.84 %ºC^{-1} for q_2 for our experimental conditions.

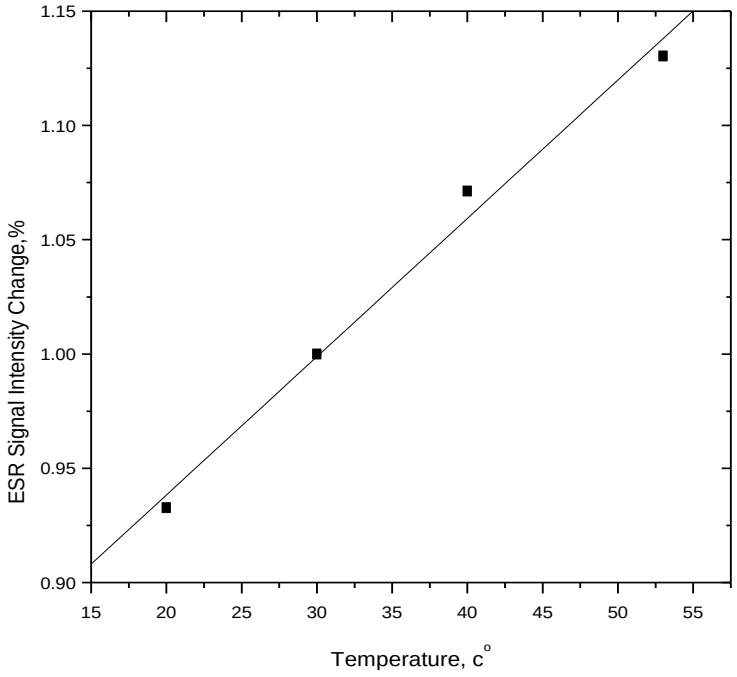

Figure 4: Variation of response of quartz rods (q_1) of concentration 20%, as a function of temperature during irradiation relative to to that at 30^0C.Irradiation dose= 5 KGy.

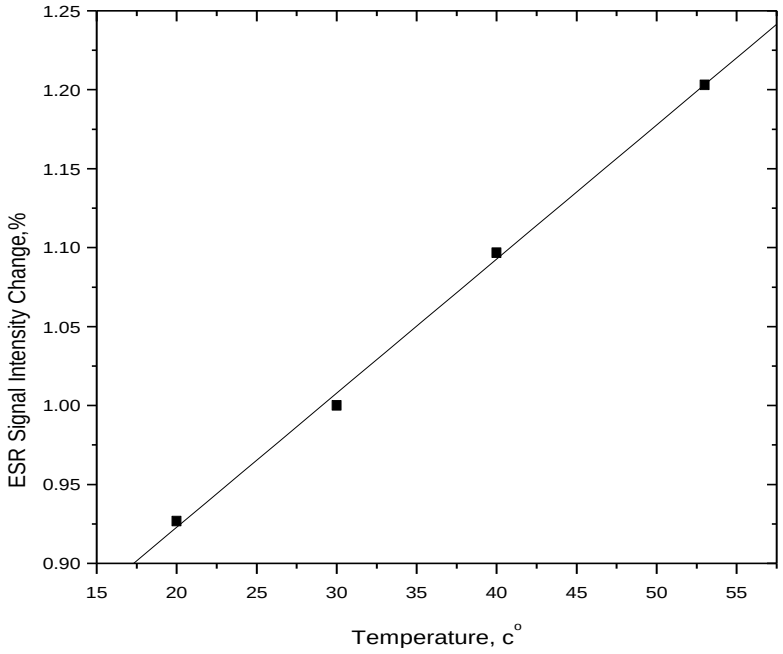

Figure 5: Variation of response of quartz rods (**q_2**) of concentration 20%, as a function of temperature during irradiation relative to to that at 30^0C.Irradiation dose= 5 KGy.

Humidity during Irradiation

The effect of relative humidity (RH) during irradiation on the response of **q_1**,**q_2** rods was investigated by irradiating the rods to a dose of 5 kGy at different relative humidity (0, 11, 33, 54, 76 and 92 %) using saturated salt solutions. The rods were stored before irradiation for a 48-h period under the same RH conditions as when irradiated, so that equilibrium moisture content in the dosimeter could be established during irradiation. Figure 6&7 show the variation in response [peak height/ (gain*mass)] as a function of percentage relative humidity during irradiation

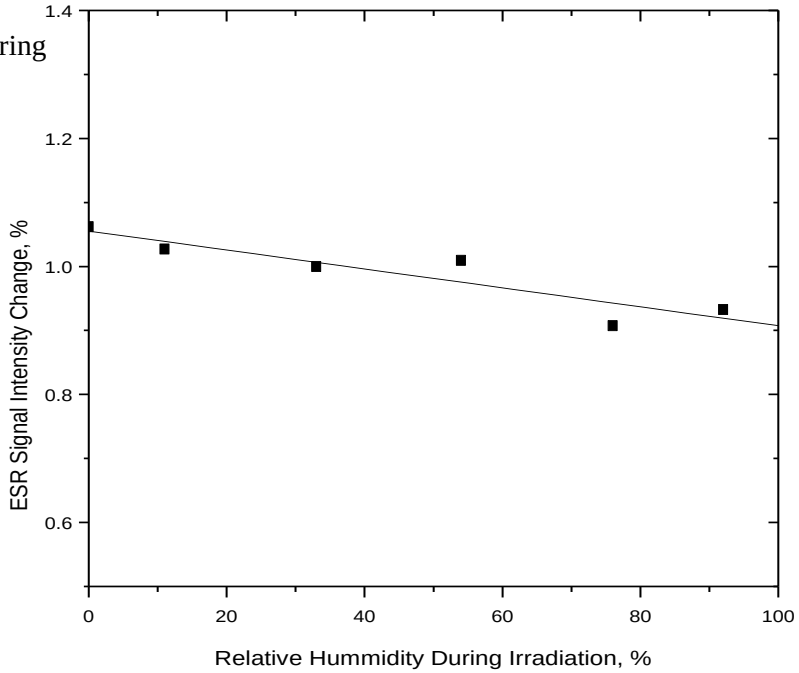

relative to that at 33%. It can be seen that the response is almost flat from 0 up to 60% RH and shows a tendency decrease at higher RH values for q_1 and from 0 up to 92% for $\mathbf{q_2}$. This result reflects the insignificant dependence of these rod dosimeters on the change of relative humidity during irradiation.

Figure 6: Variation of ESR response of quartz rods, $\mathbf{q_1}$ (conc. 20 %) as a function of relative humidity during irradiation relative to response value at 33 % relative humidity. Irradiated dose=5 KGy.

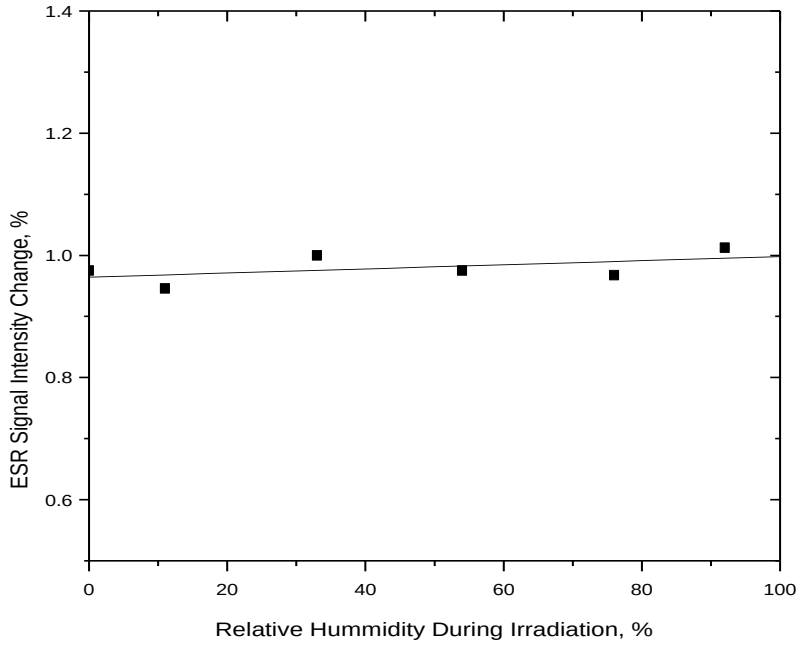

Figure 7: Variation of ESR response of quartz rods, $\mathbf{q_2}$ (conc. 20 %) as a function of relative humidity during irradiation relative to response value at 33 % relative humidity. Irradiated dose=5 KGy.

Uncertainty

Factors contributing to the total uncertainty may be separated into two types, type A and type B. Type A is evaluated by the statistical analysis of a series of observations and type B is evaluated by means other than the statistical analysis of a series of observations [11].

Sources of uncertainty for the measurement of absorbed dose by Quartz dosimeters may include the uncertainty in the absorbed dose received by the dosimeters during calibration, analysis of dosimeter response, uncertainty associated with measurement of response and fit of dosimetry data to calibration curve. Table 2&3 show the overall uncertainty for the calibration of $\mathbf{q_1}$, $\mathbf{q_2}$ dosimeters. The combined uncertainty (at two standard deviations, i.e. 2 σ, approximately equal to a 95% confidence level) is found by multiplication of U_c (at 1 σ) by two. Hence, the combined uncertainty at 2σ using $\mathbf{q_1}$ rods is 4.55 % and 5.95% for $\mathbf{q_2}$.

Table (3). Different uncertainty sources and its values arise during dose measurement using q_1 rods with concentration of 20 % for dose range 0.1 – 15 kGy.

Source of uncertainty	*Type of uncert-ainty*	*Divisor*	*Uncerta-inty value*
Calibration irradiation dose rate	**B**		**1.1450**
irradiation facility	**B**		**0.44000**
Stability of EPR during measurements	**A**	**√3**	**0.70453**
Reproducibility of EPR	**A**	**√3**	**0.81638**

Angular positioning of the quartz rod (orientation)	**A**	**√3**	**0.44578**
Vertical positioning of the sample in the cavity	**A**	**√3**	**0.68683**
Sensitivity variation (uniformity)	**A**	**√3**	**0.81530**
Uncertainty from fitting of response to absorbed dose as determined from the variation of the residuals by using third polynomial equation	**A**		**0.45600**
Uncertainty associated with measurement of rods response curve (3 rods at each absorbed dose)	**A**	**√3**	**0.57600**
Irradiation temperature	**B**	**√3**	**0.11500**
Combined standard uncertainty (u_c)			**2.13437**
Expanded uncertainty			**4.5555**

Table (4). Different uncertainty sources and its values arise during dose measurement using q_2 rods with concentration of 20 % for dose range 0.1 – 25 kGy.

Source of uncertainty	*Type of uncert-ainty*	*Divisor*	*Uncerta-inty value*
Calibration irradiation dose rate	**B**		**1.1450**
irradiation facility	**B**		**0.44000**
Stability of EPR during measurements	**A**	**√3**	**0.88710**
Reproducibility of EPR	**A**	**√3**	**0.95872**
Angular positioning of the quartz rod (orientation)	**A**	**√3**	**0.82714**

Vertical positioning of the sample in the cavity	**A**	**√3**	**0.85842**
Sensitivity variation (uniformity)	**A**	**√3**	**0.75241**
Uncertainty from fitting of response to absorbed dose as determined from the variation of the residuals by using third polynomial equation	**A**		**0.54300**
Uncertainty associated with measurement of rods response curve (3 rods at each absorbed dose)	**A**	**√3**	**0.66700**
Irradiation temperature	**B**	**√3**	**0.11500**
Combined standard uncertainty (u_c)			**2.43879**
Expanded uncertainty			**5.94771**

Energy Dependence

The energy dependence of dosimeters may cause inaccuracies in the measurement of absorbed dose in a material of interest. Most of such errors arise when a dosimeter is calibrated under specific conditions with respect to radiation energy and irradiation geometry, and it is used later under conditions that are significantly different.

The EVA/PARA/quartz 20% rod dosimeters were studied for their energy sensitivity to ionizing photons in the energy range 10 keV to 20 MeV. The mass attenuation coefficient, μ/ρ, the mass energy-absorption coefficient, μ_{en}/ρ, and the collision stopping powers, $(1/\rho.dE/dX)_{coll}$, have been calculated as a function of photon energy for the EVA/PARA/quartz 20% rod dosimeters. These calculations were based on the data available online at NIST physical reference data **internet web site [12,13]. Figs. 8-11 show the calculated attenuation coefficients, absorption coefficients and stopping powers of the EVA/PARA/quartz 20% rods, respectively, compared with the values of the adipose tissue published in the same web site. It can be seen that the ratios of $(\mu/\rho)_{Adipose}/(\mu/\rho)_{EVAPA20}$ and $(\mu_{en}/\rho)_{Adipose}/(\mu_{en}/\rho)$ EVA/PARA/quartz 20% are almost equal to unity in the photon energy range from 0.1 to 20 MeV and show a noticeable decrease at lower photon energies. On the other hand the ratio of stopping power of adipose to EVA/PARA/quartz 20% rods is almost unity overall the studied photon energy range (0.01-20 MeV). To concludes, energy dependence of these rod dosimeters is insignificant over 100 keV.**

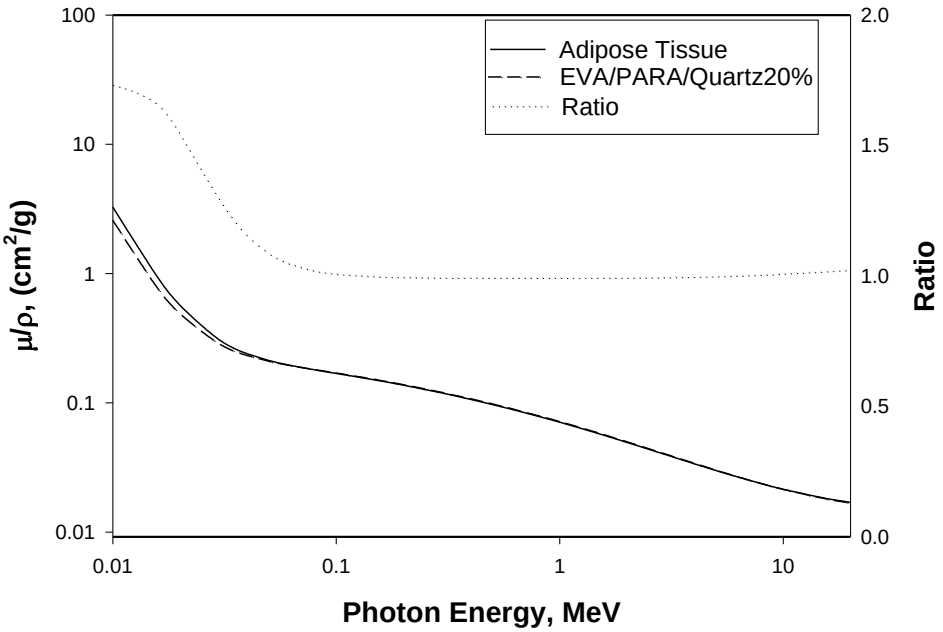

Figure 8 left ordinate: Calculated mass-energy attenuation coefficients of Quartz and Adipose tissue versus photon energy . Right ordinate : Ratio of attenuation coefficients versus photon energy.

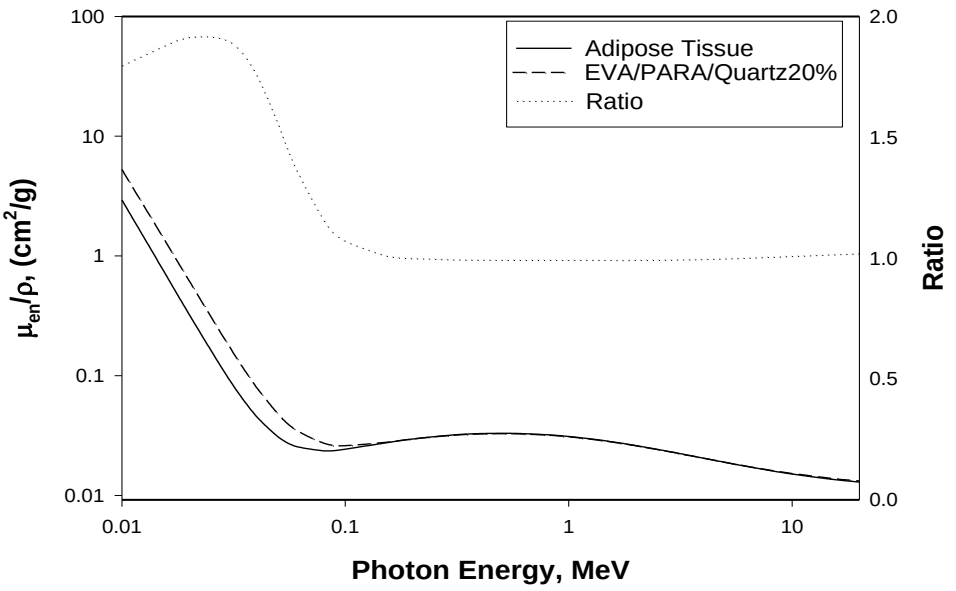

Figure 9 Left ordinate: Calculated mass –energy absorption coefficients of Quartz and Adipose tissue versus photon energy. Right ordinate: Ratio of absorption coefficients versus photon energy.

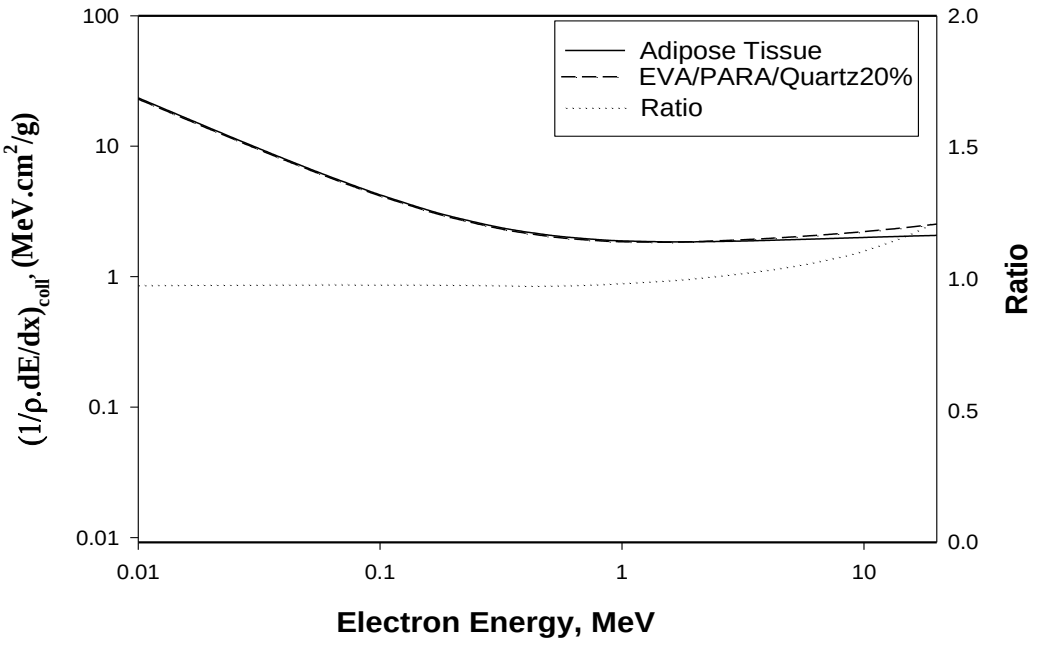

Figure 11: Left ordinate: Calculated collision mass stopping powers of EVAPA20 and Adipose tissue versus photon energy. Right ordinate: Ratio of absorption coefficients versus Electron energy.

Stability at Different Storage Conditions

The post-irradiation stability has been studied for 9 sets of Quartz rods (q_1, q_2 each set consists of 3 rods) for a period of 150 days. 3 sets were irradiated to a dose of 25 kGy and stored in dark at different temperatures (namely, 0, 25 and 40 ºC). Figs. 12&13 show the relative peak-to-peak signal height as a function of post-irradiation storage time. It can be seen that these rods are fairly stable after irradiation and also the response increases inversely with the storage temperature in dark over the 150-day storage period.

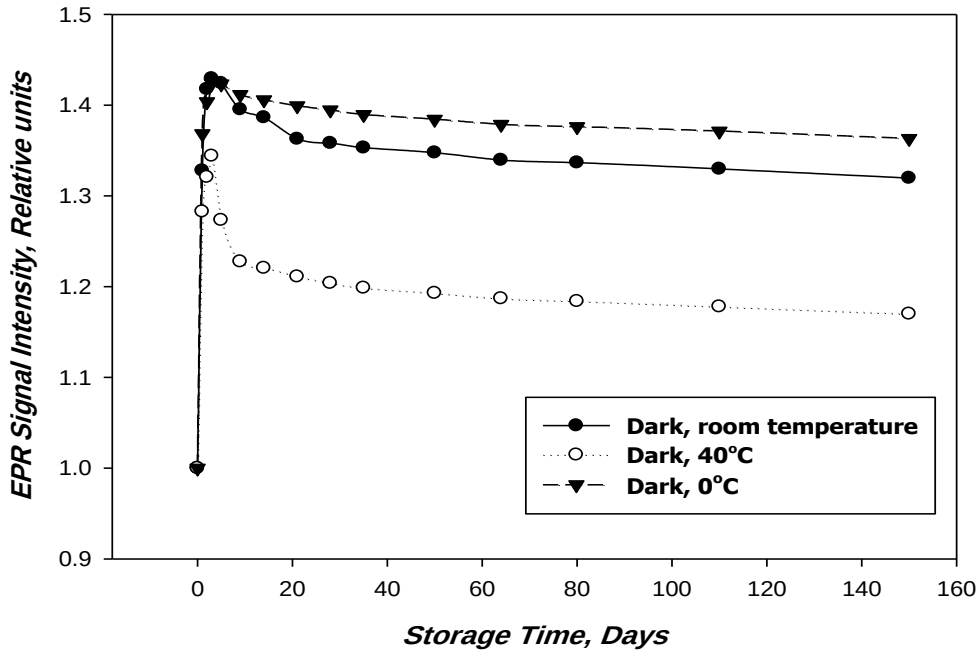

Figure (12): Decay of EPR lines of irradiated quartz rods (q_1) at different storage conditions (dose = 25 kGy)

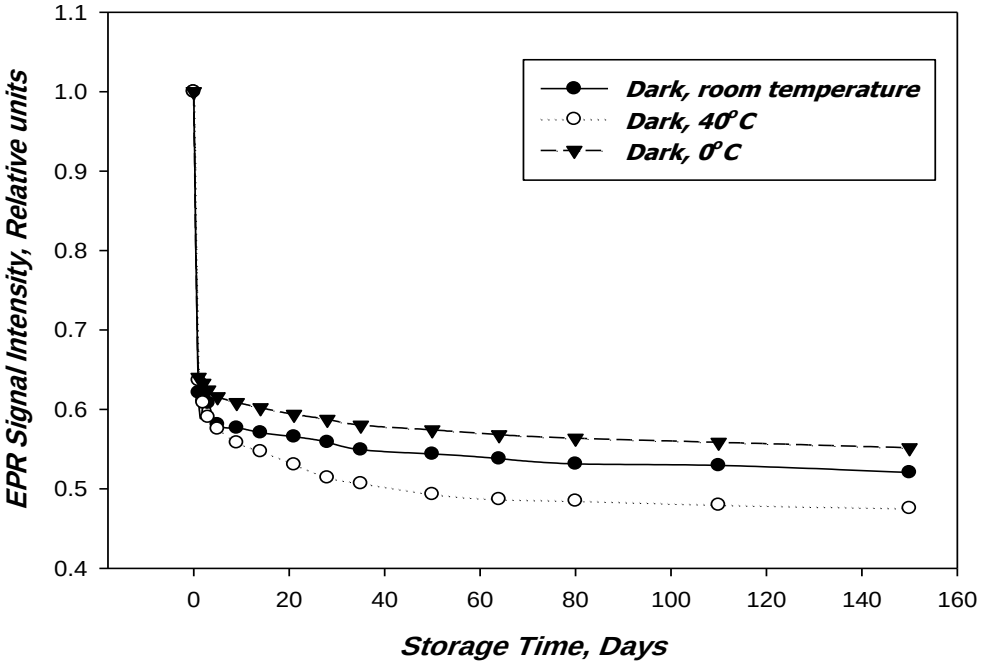

Figure (13): Decay of EPR lines of irradiated quartz rods (**q_2**) at different storage conditions (dose = 25 kGy)

CONCLUSIONS

From the data presented in this paper, the following conclusions can be drawn:

1- ***A new quartz-EPR rod dosimeter has been prepared by a simple technique in the laboratory using ethylene vinyl acetate copolymer and paraffin wax as binding materials.***

2- ***The prepared rods have good mechanical properties adequate for easy and safe handling.***

3- ***The quartz rods can be used with good precision in the dose range from 0.1 to 15 kGy for q_1 and 0.1 to 25 KGy for q_2.***

4- ***The temperature coefficient was found to be +0.6 % $^oC^{-1}$ for q_1 and 0.84% $^oC^{-1}$ for q_2.***

5- ***These rods dosimeter have insignificant dependence on the change of relative humidity during irradiation.***

6- The overall uncertainty for calibration of the EVAPA rod dosimeters at 2σ was found to be 4.55 % for q_1 and 5.95% for q_2.

7- Energy dependence of these rod dosimeters is insignificant over 100 keV.

8- These dosimeters are fairly stable after irradiation and show a little fading between over 150-day storage period depending on irradiation dose and storage condition.

REFERENCES

[1] D.F. Regulla and U. Deffner, Int. J. Appl. Radiat. Isotp., 33, 1101(1982).
[2] T. Kojima, R.Tanaka, Y.Morita and T. Seguchi, Appl. Radiat. Isotp., 37, 517(1986).
[3] Kojima, T. Ranjith, H. Haruyama, Y. Kashiwazaki and R. Tanaka, Appl. *Radiat.* Isot., 44, 41(1993).
[4] K.W. Hansen, K.J. Olsen and M. Wille, Radiat. Protect. Dosim., 19, 43(1987).
[5] Janovsky, I. Harsen and P.Cernoch, Appl. Radiat. Isot., 39, 651(1988).
[6] D.F. Regula, A. Scharmann and W.L. McLaughlin, *ESR* Dosimetry and Applications., 23, 534(1989).
[7] T. Kojima and R. Tanaka, Appl. Radiat. Isot., 40, 851(1989).
[8] Bartolotta, A. Indovina, P.L. Onori and A. Rosati, Radiat. Protect. Dosim., 9, 277(1984).
[9] J.M. Arber and P.H. Sharpe, Appl. Radiat. Isot., 44, 19(1993).
[10] M.T. Razzak, S. Sudiro, A. Sudradjat, A. Waskito and M.F. Djamili, Radiat. Phys. Chem., 46, 1263-1267(1995).
[11] ASTM, American Society for Testing and Materials, Annual Book of ASTM Standards, Standard Guide E 1707(2002).
[12] Hubbell, J. H. and Seltzer, S. M. (1997). Tables of X-Ray Mass Attenuation Coefficients and Mass Energy-Absorption Coefficients (version 1.03), [Online]. Available: http://physics.nist.gov/xaamdi. National Institute of Standards and Technology, Gaithersburg, MD.
[13] Berger, M. J., Coursey, J. S., and Zucker, M. A. (1999). ESTAR, PSTAR, and ASTAR: Computer Programs for Calculating Stopping-Power and Range Tables for Electrons, Protons, and Helium Ions (version 1.21), [Online]. Available: http://physics.nist.gov/Star. National Institute of Standards and Technology, Gaithersburg, MD.